Turk J Elec Engin, VOL.15, NO.2 2007, © TÜBİTAK

Aggregation, Foraging, and Formation Control of Swarms with Non-Holonomic Agents Using Potential Functions and Sliding Mode Techniques*†

Veysel GAZİ[1], Barış FİDAN[2], Y. Sinan HANAY[1] and M. İlter KÖKSAL[1]
[1] *Department of Electrical and Electronics Engineering, TOBB University of Economics and Technology, Söğütözü Cad. No: 43, 06560 Ankara-TURKEY*
e-mail: {vgazi, hanay, i.koksal}@etu.edu.tr
[2] *National ICT Australia Ltd. and The Australian National University, Research School of Information Sciences & Engineering, Canberra-AUSTRALIA*
e-mail: Baris.Fidan@anu.edu.au

Abstract

In this article we consider the aggregation, foraging, and formation control of swarms whose agents are moving in 2-dimensions with non-holonomic unicycle agent dynamics. We approach these problems using artificial potentials and sliding mode control. The main contribution is extension of the recent results (mainly for aggregation) in the literature based on a similar approach for simple integrator agent dynamics models to a significantly more realistic and more difficult setting with non-holonomic unicycle agent dynamics models. In particular, we design continuous-time control schemes via a constructive analysis based on artificial potential functions and sliding mode control techniques. The effectiveness of the proposed designs are demonstrated analytically as well as via a set of simulation results.

1. Introduction

Coordination and control of multi-agent systems including swarms have attracted considerable attention recently, in parallel with the interest in applications of such systems in various areas involving groups of robots, mobile sensors, manned or unmanned aerial, ground, space, or underwater vehicles, etc. [1–8]. Beside the usual requirement of decentralized decision making, the swarm coordination and control problems and approaches are significantly diverse depending on the considered agent dynamics, specific control goals and strategies, inter-agent information structure, etc. A brief survey on such problems and approaches is given in [9].

In this paper we consider the *aggregation*, *foraging*, and *formation control* of swarms whose agents are moving in 2-dimensions with non-holonomic unicycle agent dynamics. We approach these problems using artificial potentials and sliding mode control.

*A condensed version of this paper containing a subset of the results presented here appeared at the European Control Conference (ECC 2007), Kos, Greece.

†The work of V. Gazi, Y. S. Hanay, M. İ. Köksal is supported by TÜBİTAK (the Scientific and Technological Research Council of Turkey) under grant No. 104E170 and by the European Commission under FP 6 contract No. 045203 (the GUARDIANS project). The work of B. Fidan is supported by National ICT Australia, which is funded by the Australian Government's Department of Communications, Information Technology and the Arts and the Australian Research Council through the *Backing Australia's Ability* initiative and the ICT Centre of Excellence Program.

Aggregation (or gathering together) is a basic behavior exhibited by many swarms in nature, including simple bacteria colonies, flocks of birds, schools of fish, and herds of mammals. Such behavior of biological swarms is observed to be helpful in meeting various tasks such as avoiding predators, increasing the chance of finding food, etc. [10]. This can be explained by the relative appropriateness of an aggregated swarm structure to meet these tasks collaboratively as compared to a non-aggregated setting. Because of the same reason, aggregation is a desired behavior in engineering multi-agent dynamic systems as well. Moreover, many of the collective behaviors seen in biological swarms and some behaviors to be possibly implemented in engineering multi-agent dynamic systems emerge in aggregated swarms. Therefore, studying the dynamics and properties of swarm aggregations is important in developing efficient cooperative multi-agent dynamic systems.

Aggregation in biological swarms were initially modelled and simulated by biologists [11–14]. Inspired by these works, a recent series of studies [15–22] has provided rigorous stability and convergence analysis of swarm aggregations based on artificial potential functions both with continuous-time and discrete-time formulations. Particularly, in [15,16] a biologically inspired n-dimensional (where n is arbitrary) continuous time synchronous swarm model based on artificial potentials is considered and some results on cohesive swarm aggregation have been obtained. Similar results based on artificial potentials and virtual leaders have been independently obtained by Leonard and coworkers in [23, 24] for agents with point mass dynamics. The papers [19–21] focus on asynchronous swarm models with time delays for swarm aggregation in discrete-time settings.

In [22], which has more emphasis on design than analysis as opposed to the papers mentioned in the previous paragraph, a particular control strategy for swarm aggregations has been developed based on artificial potential functions and sliding mode control, assuming simple integrator agent dynamics with model uncertainties and disturbances. One particular contribution of this paper is extension of the results in [22] to a significantly more realistic and more difficult setting with non-holonomic unicycle agent dynamics models, again using the tools of artificial potential functions and sliding mode control, but in a slightly different way than [22]. Moreover, we provide similar control schemes for *foraging* and *formation control* of swarms, under the same assumption of non-holonomic unicycle agent dynamics and employing the same artificial potential and sliding mode control tools.

Foraging can be considered as a constrained form of aggregation, where the environment affects the motion or behavior of agents. The environment may have favorable regions (representing targets or goals) to which the agents may want or need to move, and unfavorable regions (representing threads or obstacles) which the agents may want or need to avoid. Hence, for a foraging task, the swarm coordination and control scheme to be developed need to guarantee aggregation in the favorable regions while avoiding unfavorable ones.

In this paper we consider *formation control* as a special form of swarm aggregation, where the final aggregated form of the swarm is desired to constitute a particular predefined geometrical configuration that is defined by a set of desired inter-agent distance values. This is achieved by defining the potential function to achieve its global minimum at the desired formation. For this case, however, due to the fact that potential functions may have many local minima, the results obtained are usually local. In other words, unless the potential function is defined to have a single (unique) minimum at the desired formation, convergence to that formation is guaranteed only if the agents start from a "sufficiently close" configuration or positions to the desired formation.

Artificial potential functions have been used extensively for robot navigation and control, see e.g. [25, 26]. There exist a number of more recent studies on applications of artificial potentials to multi-agent

system coordination and cooperative control [2, 27]. There is also a relevant literature on formation control of autonomous vehicles [3, 28–33] as well as control and analysis of flocking behavior [34–37], where artificial potential functions are used together with a number of other techniques including some graph theoretical and Lyapunov analysis based ones. Some of these works are based on point mass agent dynamics [2, 27, 31, 33–36], while others use non-holonomic agent dynamics [3, 28–30, 37].

Sliding mode control [38], which is the main technique we use in our work in addition to artificial potential functions, is an important technique that has been used extensively in various areas including navigation of vehicles and mobile robots [39–44]. The wide use of this technique for various tracking control problems is mainly because it is a robust technique which guarantees that the tracking is achieved in the existence of uncertainties and disturbances in the system dynamics.

In [39–41], sliding mode control is used for navigation of holonomic robots and obstacle avoidance in an environment modeled using harmonic potentials. In [42–44] the strategy is extended to navigation of robots with non-holonomic dynamics as well. The strategy in these works is based on forcing the motion of the robot along the gradient of the potential field representing the environment. In [22], a similar procedure is applied for implementation of a class of engineering aggregating swarm models composed of robots with fully actuated (holonomic) motion dynamics. As mentioned earlier, in this paper, we extend the study in [22] to swarms consisting of agents with non-holonomic unicycle vehicle dynamics.

The rest of the paper is organized as follows. In Section 2, we present the non-holonomic agent dynamics model we are assuming in our work and formally define the swarm aggregation problem to be investigated. In Sections 3 and 4, we present our control design for the aggregation problem defined in 2 based on artificial potential fields and sliding mode control. We give formal definitions of the particular foraging and formation control tasks we investigate in this paper and present our corresponding control designs in Sections 5 and 6, respectively. In Section 7, we demonstrate the effectiveness and characteristics of our designs via simulation examples. The paper is concluded with some final remarks in Section 8.

2. Swarm Aggregation Problem with Non-Holonomic Agents

Consider a system of N hon-holonomic mobile agents, e.g. robots, moving in $\mathbb{R}^2$ that are labelled as $A_1, \ldots, A_N$. Assume that each agent A_i $(i = 1, \ldots, N)$ has the configuration depicted in Figure 1 and the equations of motion given by

$$\begin{aligned} \dot{x}_i &= v_i \cos(\theta_i), \\ \dot{y}_i &= v_i \sin(\theta_i), \\ \dot{\theta}_i &= w_i, \\ \dot{v}_i &= \tfrac{1}{m_i} F_i, \\ \dot{w}_i &= \tfrac{1}{I_i} \tau_i \end{aligned} \tag{1}$$

where x_i and y_i are the Cartesian coordinates, θ_i is the steering angle, v_i is the linear speed, and w_i is the angular speed of A_i. The quantities m_i and I_i are positive constants and represent the mass and the moment of inertia of the agent A_i, respectively. The control inputs for the agent A_i are the force input F_i and the torque input τ_i. Note that this model includes both kinematic and dynamic equations for each agent, i.e., it includes the (linear and angular) velocity dynamics in addition to the agent kinematics. This is equivalent to adding two integrators to the kinematic model.

In this article we are concerned with the problems of aggregation, foraging, and formation control for the agents with the dynamics given in (1). In other words, we would like to design the control inputs $u_{i1} = F_i$

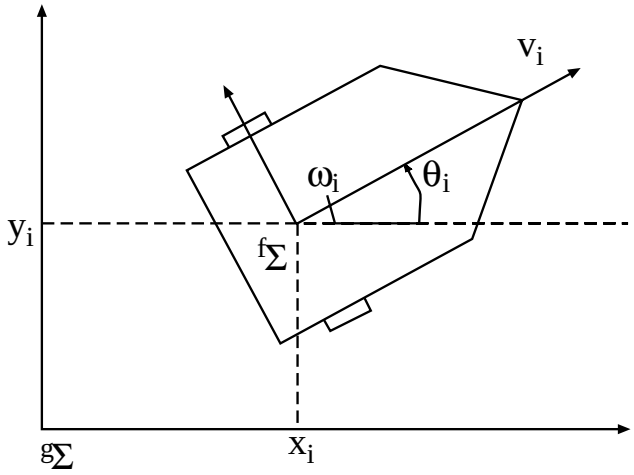

Figure 1. The unicycle robot.

and $u_{i2} = \tau_i$ such that the system of N agents with the non-holonomic dynamics given in (1) and with (possibly) arbitrary initial positions depending on the objective aggregate (gather together), successfully forage by collectively moving to favorable regions and avoiding unfavorable regions of the environment, or achieve a predefined desired geometrical shape (a formation).

First we start with the aggregation problem of the agents and investigate it in the following two sections (Sections 3 and 4). The foraging and the formation control problems are investigated after that in Sections 5 and 6, respectively. Denoting the position of each agent A_i $(i = 1, \ldots, N)$ by $p_i = [x_i, y_i]^\top$, we can formulate the aggregation control problem as follows.

Problem 1 (Aggregation) *Design the control inputs* $u_i = [u_{i1}, u_{i2}]^\top$ *for each agent* $A_i, i = 1, \ldots N$, *such that for some* $\epsilon > 0$ *as* $t \to \infty$ *we have*

$$p_i \to B_\epsilon(p_c) \tag{2}$$

where $p_c = \frac{1}{N}\sum_{i=1}^{N} p_i$ *is the centroid of the swarm and* $B_\epsilon(p_c) = \{p \in \mathbb{R}^2 : \|p - p_c\| \leq \epsilon\}$ *is the disk with radius* ϵ *around the centroid* p_c.

Note that this problem can be formulated also as

$$\lim_{t\to\infty} \|p_i - p_j\| \leq 2\epsilon$$

for all i and j. Here the size of the swarm (or the gathering area) ϵ is a design parameter that can be chosen by the system designer. Note that for the above problem definition it is assumed that the agents have point dimensions (although moving with non-holonomic constraints). If the agents have certain predefined occupation areas (size or dimension), then the swarm size ϵ cannot be chosen arbitrarily small and should be consistent with the number of agents and the area each agent occupies. For such cases there is a need to choose the potential function appropriately and it is possible to obtain lower bounds on the size of the swarm which depends on the occupation areas of the agents [16].

3. Artificial Potential Functions

In our approach to Problem 1, we use artificial potential functions in order to construct attractive-repulsive relations among the agents. In other words, our design procedure is based on a potential function which is selected such that the corresponding potential field is attractive for agent pairs with large inter-agent distances (in order to result in aggregation) and repulsive for short inter-agent distances (in order to avoid collisions between the robots). In our work, we use a particular potential function of the form considered in [15–17].

In [15, 16] it was shown for a certain class of potential functions $J(p)$ that if the agents move in the space $\mathbb{R}^n$ based on

$$\dot{p}_i = -\nabla_{p_i} J(p), \tag{3}$$

where $J : \mathbb{R}^{nN} \to \mathbb{R}$ is the potential function, $p = [p_1^\top, \ldots, p_N^\top]^\top \in \mathbb{R}^{nN}$ is the lumped vector of the positions $p_i \in \mathbb{R}^n$ of the agents A_i $(i = 1, \ldots, N)$, then aggregation in the form defined in Problem 1 will be achieved. The potential functions considered in [15, 16] satisfy

$$\nabla_{p_i} J(p) = \sum_{j=1, j\neq i}^{N} g(p_i - p_j), \; i = 1, \ldots, N \tag{4}$$

where $g : \mathbb{R}^n \to \mathbb{R}^n$ are odd functions (called attraction/repulsion functions) that represent the attraction and repulsion relationships between the individuals. Moreover, it was assumed that for any $\bar{p} \in \mathbb{R}^n$, $g(\bar{p})$ satisfies

$$g(\bar{p}) = -\bar{p}[g_a(\|\bar{p}\|) - g_r(\|\bar{p}\|)],$$

where $g_a(\|\bar{p}\|)$ represents the attractive part which dominates on large distances and $g_r(\|\bar{p}\|)$ represents the repulsive part which dominates on short distances. One potential function which satisfies these assumptions and was used in [15, 17] is

$$J(p) = \sum_{i=1}^{N-1} \sum_{j=i+1}^{N} \left[\frac{a}{2} \|p_i - p_j\|^2 + \frac{bc}{2} \exp\left(-\frac{\|p_i - p_j\|^2}{c} \right) \right], \tag{5}$$

for which (4) is satisfied with

$$g(p_i - p_j) = (p_i - p_j) \left[a - b \exp(-\frac{\|p_i - p_j\|^2}{c}) \right] \tag{6}$$

where a, b and c are positive scalars that need to be chosen appropriately. In particular, we need $b > a$ in order to achieve short range repulsion. Note that for the potential function in (5) the size of the gathering region in Problem 1 is given by

$$\epsilon = \frac{b}{a} \sqrt{\frac{c}{2}} \exp\left(-\frac{1}{2} \right).$$

Note also that the above value of ϵ is a very conservative bound obtained as a result of a Lyapunov analysis and in reality the actual swarm size is much smaller than it. Therefore, beside the value of ϵ another parameter that may give information about the size of the swarm could be the distances at which the

attraction and repulsion between two individuals balance. For the potential function in (5) this happens at the distance

$$\delta = \sqrt{c \ln\left(\frac{b}{a}\right)},$$

which is obtained by equating (6) to zero.

In this article, we also utilize the potential function in (5). However, we would like to emphasize that the procedure is not limited to that potential function only and can be used with other potential functions as well. Note also that in our case $p = [p_1^\top, \ldots, p_N^\top]^\top \in \mathbb{R}^{2N}$ and $p_i = [x_i, y_i]^\top \in \mathbb{R}^2$ for $i = 1, \ldots, N$).

4. Sliding Mode Control for Swarm Aggregation

As mentioned in Section 1, sliding mode control is a widely used technique in various application areas, mainly because of its suppressive and robust characteristics against the uncertainties and the disturbances in the system dynamics. The shortcomings (of the raw form of the sliding mode control scheme) on the other hand are the so-called chattering effect and possible generation of high-magnitude control signals. Note that these shortcomings may possibly be avoided or relaxed via integration and some filtering techniques.

In sliding mode control, a switching controller with high enough gain is applied to suppress the effects of modelling uncertainties and disturbances, and the agent dynamics are forced to move along a stabilizing manifold, which is also called a *sliding manifold*. The value of the gain is computed using the known bounds on the uncertainties and disturbances.

In this section, we design a sliding mode control scheme to solve Problem 1 via forcing the motion of each individual agent along the negative gradient of the potential $J(p)$ in (5), i.e. forcing each agent to obey equation (3) where J is as defined in (5). This will lead to recovering the aggregation behavior (of the single-integrator dynamics) obtained in [15] for swarms consisting of agents with the non-holonomic agent dynamics in (1).

Let

$$-\nabla_{p_i} J(p) = \begin{bmatrix} -J_{x_i}(p) \\ -J_{y_i}(p) \end{bmatrix}$$

denote the gradient of the potential at p_i. In order to achieve satisfaction of (3) we need

$$-\nabla_{p_i} J(p) = \begin{bmatrix} -J_{x_i}(p) \\ -J_{y_i}(p) \end{bmatrix} = \begin{bmatrix} v_i \cos\theta_i \\ v_i \sin\theta_i \end{bmatrix}. \tag{7}$$

In other words, we need

$$v_i = \|\nabla_{p_i} J(p)\|, \quad \theta_i = \arctan\left(\frac{J_{y_i}(p)}{J_{x_i}(p)}\right) (\text{mod}360^\circ). \tag{8}$$

Note that since the inputs in the agent model (1) are $u_{i1} = F_i$ and $u_{i2} = \tau_i$, i.e. v_i and θ_i cannot be applied directly, the terms

$$v_{id} \triangleq \|\nabla_{p_i} J(p)\|, \quad \theta_{id} \triangleq \arctan\left(\frac{J_{y_i}(p)}{J_{x_i}(p)}\right) (\text{mod}360^\circ) \tag{9}$$

need to be considered as desired set-point values for v_i and θ_i, respectively.

Our objective is to force the motion of the agents such that the differences $(v_i - v_{id})$ and $(\theta_i - \theta_{id})$ converge to zero. With this objective in mind, similar to [42–44], let us define two sliding surfaces [38], one for the translational speed v_i and one for the orientation θ_i, respectively, as

$$s_{v_i} = v_i - v_{id} \tag{10}$$

$$s_{\theta_i} = c(\dot{\theta}_i - \dot{\theta}_{id}) + (\theta_i - \theta_{id}), \tag{11}$$

where $c > 0$ is a positive constant. With these definitions, our objective becomes to design the control inputs u_{i1} and u_{i2} so that $s_{v_i} \to 0$ and $s_{\theta_i} \to 0$ asymptotically, since if they are achieved we will have $v_i \to v_{id}$ and $\theta_i \to \theta_{id}$. Note here that the existence of the additional term $c(\dot{\theta}_i - \dot{\theta}_{id})$ in (11) is because of the double integrator relationship between θ_i and the applicable input $u_{i2} = \tau_i$ as opposed to the single integrator relationship between v_i and $u_{i1} = F_i$.

It is well known from the sliding mode control theory that if we have the reaching conditions

$$s_{v_i}\dot{s}_{v_i} \leq -\varepsilon_1 |s_{v_i}| \tag{12}$$

$$s_{\theta_i}\dot{s}_{\theta_i} \leq -\varepsilon_2 |s_{\theta_i}| \tag{13}$$

satisfied for some constants $\varepsilon_1, \varepsilon_2 > 0$, then $s_{v_i} = 0$ and $s_{\theta_i} = 0$ will be achieved in finite time.

Now let us assume that $|\dot{v}_{id}| \leq \alpha(p)$ for some known $\alpha(p) > 0$. The properties of such $\alpha(p)$ depend on the properties of the potential function, which is chosen by the designer. In other words, one can choose the potential function such that such $\alpha(p)$ exists. For example, for the potential function in (5) one can calculate (see the Appendix) $\alpha(p)$ as

$$\alpha(p) = 2\bar{\alpha}(p) \max_{i \in \{1,\dots,N\}} \left(\sum_{j=1, j\neq i}^{N} \|G(p_i - p_j)\| \right),$$

where

$$\bar{\alpha}(p) = \max_{k \in \{1,\dots,N\}} \left(\|\nabla_{p_k} J(p)\| + s_{v_k}(0) \right).$$

and

$$G(p_i - p_j) = \\ aI + b \exp\left(-\frac{\|p_i - p_j\|^2}{c} \right) \left(\frac{2}{c}(p_i - p_j)(p_i - p_j)^\top - I \right).$$

In order to achieve the satisfaction of (12) we choose the first control input $u_{i1} = F_i$ as

$$u_{i1} = -K_{i1}\mathrm{sgn}(s_{v_i}) \tag{14}$$

using which the time derivative of s_{v_i} becomes

$$\dot{s}_{v_i} = -\frac{K_{i1}}{m_i}\mathrm{sgn}(s_{v_i}) - \dot{v}_{id}$$

and we have

$$s_{v_i}\dot{s}_{v_i} = s_{v_i}\left(-\frac{K_{i1}}{m_i}\text{sgn}(s_{v_i}) - \dot{v}_{id}\right) = -\frac{K_{i1}}{m_i}|s_{v_i}| - s_{v_i}\dot{v}_{id} \leq -\left(\frac{K_{i1}}{m_i} - \alpha(p)\right)|s_{v_i}| \tag{15}$$

Then by choosing K_{i1} according to

$$K_{i1} \geq m_i(\alpha(p) + \varepsilon_1) \tag{16}$$

one guarantees that (12) is satisfied and sliding mode occurs (i.e., $s_{v_i} = 0$ is satisfied) in finite time.

Similarly, for the second sliding surface choosing the control input as

$$u_{i2} = -K_{i2}\text{sgn}(s_{\theta_i}) \tag{17}$$

the time derivative of s_{θ_i} becomes

$$\dot{s}_{\theta_i} = -c\frac{K_{i2}}{I_i}\text{sgn}(s_{\theta_i}) - c\ddot{\theta}_{id} + \omega_i - \dot{\theta}_{id} \tag{18}$$

and we have

$$s_{\theta_i}\dot{s}_{\theta_i} = s_{\theta_i}\left(-\frac{cK_{i2}}{I_i}\text{sgn}(s_{\theta_i}) - c\ddot{\theta}_{id} + \omega_i - \dot{\theta}_{id}\right) \leq -\left(\frac{cK_{i2}}{I_i} - c|\ddot{\theta}_{id}| - |\dot{\theta}_{id}| - |\omega_i|\right)|s_{\theta_i}| \tag{19}$$

By choosing K_{i2} as

$$K_{i2} \geq \frac{I_i}{c}\left(c|\ddot{\theta}_{id}| + |\dot{\theta}_{id}| + |\omega_i| + \varepsilon_2\right) \tag{20}$$

one can guarantee that (13) is satisfied and the second sliding surface $s_{\theta_i} = 0$ in (11) will as well be reached in finite time.

In order to be able to compute the value of s_{θ_i} one needs the time derivative of θ_{id}. Taking its derivative with respect to time we obtain

$$\dot{\theta}_{id} = \frac{\frac{d}{dt}\left(\frac{J_{y_i}}{J_{x_i}}\right)}{1 + \left(\frac{J_{y_i}}{J_{x_i}}\right)^2} = \frac{\frac{d}{dt}\left(J_{y_i}\right)\cdot J_{x_i} - \frac{d}{dt}\left(J_{x_i}\right)\cdot J_{y_i}}{\left(J_{x_i}\right)^2\left(1 + \left(\frac{J_{y_i}}{J_{x_i}}\right)^2\right)} = \frac{\frac{d}{dt}\left(J_{y_i}\right)\cdot J_{x_i} - \frac{d}{dt}\left(J_{x_i}\right)\cdot J_{y_i}}{\left(J_{x_i}\right)^2 + \left(J_{y_i}\right)^2} \tag{21}$$

For the potential function in (5) we have

$$\frac{d}{dt}\left(J_{x_i}\right) = \sum_{j=1,j\neq i}^{N}\Bigg[-\left[a - b\left(1 - \frac{2(x_i-x_j)^2}{c}\right)\exp\left(-\frac{\|p_i-p_j\|^2}{c}\right)\right](\dot{x}_i - \dot{x}_j) + \left[b\frac{2(x_i-x_j)(y_i-y_j)}{c}\exp\left(-\frac{\|p_i-p_j\|^2}{c}\right)\right](\dot{y}_i - \dot{y}_j)\Bigg]$$

and

$$\frac{d}{dt}\left(J_{y_i}\right) = \sum_{j=1,j\neq i}^{N}\Bigg[-\left[a - b\left(1 - \frac{2(y_i-y_j)^2}{c}\right)\exp\left(-\frac{\|p_i-p_j\|^2}{c}\right)\right](\dot{y}_i - \dot{y}_j) + \left[b\frac{2(x_i-x_j)(y_i-y_j)}{c}\exp\left(-\frac{\|p_i-p_j\|^2}{c}\right)\right](\dot{x}_i - \dot{x}_j)\Bigg]$$

which follow from (27) in the Appendix and are used in (21) to compute $\dot{\theta}_{id}$. Note also that $|\dot{\theta}_{id}|$ and $|\ddot{\theta}_{id}|$ (which is also a computable value) are needed in order to determine the controller gain K_{i2}.

One drawback here is that to implement the control algorithm for agent A_i one needs not only the position but also the velocity of its neighbors (which are all the other agents in the particular setting here - but this is not necessarily required to be the case in general).

We would like to also emphasize that although not explicitly considered here the procedure based on the sliding mode control technique discussed above will guarantee proper behavior even in the presence of uncertainties in the mass m_i and the inertia I_i of the robots and additive disturbances/uncertainties to the linear and angular speed dynamics which constitute very realistic assumptions.

Once the sliding mode occurs on all the surfaces (which happens in finite time) and the equation in (3) is also satisfied, based on the results in [15] we know that Problem 1 will be solved. One issue to note, however, is that after occurrence of sliding mode we reach $v_i = v_{id}$ but not necessarily $\theta_i = \theta_{id}$. In fact, after occurrence of sliding mode we have $\theta_i \to \theta_{id}$ exponentially fast and the speed of convergence depends on the slope of the sliding surface $-\frac{1}{c}$. Therefore, one needs to choose c as small as possible in order to achieve faster convergence and avoid any instabilities. Note also that decreasing the parameter c will require increasing the controller gain K_{i2}.

5. Social Foraging

Aggregation in natural swarms usually occurs during *social foraging*. Social foraging has some inherent evolutionary advantages and even simple bacteria are able to exhibit such behavior [45]. In [17] a simple model of a foraging swarm consisting of agents with simple single-integrator dynamics was considered in different environments modeled with potential functions (which we refer here as the *resource profile*). The results in [17] were later extended in [18] to agents with point mass dynamics and sensing errors/uncertainties. In this section we show that using the sliding mode control techniques discussed in the preceding sections the social foraging model in [17] can be implemented on swarms consisting of non-holonomic agents with vehicle dynamics in (1). We define the social foraging problem as follows.

Problem 2 (Social Foraging) *Consider a swarm with N agents $A_1, ..., A_N$ moving in environment $E \subset \mathbb{R}^2$ whose resource profile is represented by a continuously differentiable function $\sigma : \mathbb{R}^2 \to \mathbb{R}$. Assume that areas where $\sigma(\bar{p}) < 0$ represent favorable regions (representing nutrients in biological systems and targets or goals in engineering applications) whereas areas with $\sigma(\bar{p}) > 0$ represent unfavorable regions (representing toxic substances in biological systems and threads or obstacles in engineering applications). Design the control inputs $u_i = [u_{i1}, u_{i2}]^\top$ for each agent $A_i, i = 1, \dots N$, such that for all t the swarm does not disperse (or stays cohesive), i.e., there exists $R < \infty$ such that*

$$\|p_i - p_j\| \leq R,$$

for all t and for all pairs (i, j) and move toward favorable regions and avoid unfavorable regions.

Depending on the environment or the considered application the resource profile $\sigma(\cdot)$ may have different shapes or properties. In this article we consider one of the profiles considered in [17]. In particular, we consider a multi-modal Gaussian type of profile of the form

$$\sigma(\bar{p}) = \sum_{i=1}^{N} B_{\sigma_i} \exp\left(-\frac{\|\bar{p} - x_{\sigma_i}\|^2}{c_i}\right) \tag{22}$$

where $B_{\sigma_i} \in \mathbb{R}$ represents the strength, $x_{\sigma_i} \in \mathbb{R}^2$ represents the center, and $c_i \in \mathbb{R}^+$ represents the spread of the i^{th} Gaussian. Note that at the point $p_i = x_{\sigma_i}$ the potential function $\sigma(\bar{p})$ has an extremum (i.e. either a maximum or a minimum which depends on the sign of B_{σ_i}). Here each Gaussian with $B_{\sigma_i} < 0$ may represent a target and that with $B_{\sigma_i} > 0$ may represent an obstacle and the magnitude of B_{σ_i} may represent the priority or strength of that target or obstacle, whereas x_{σ_i} may be the position and c_i the size of that object. One particular profile of this shape is shown in Figure 2.

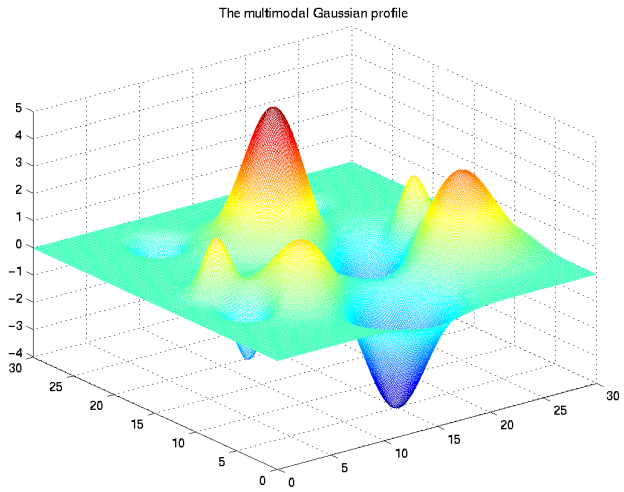

Figure 2. A Multi-Modal Gaussian environment potential (a resource profile).

In order to solve Problem 2 the total potential function is defined such that it includes the environment potential at the positions of the agents together with the inter-individual interactions potential in (5). In other words, the new potential function $J(p)$ becomes

$$J(p) = \sum_{i=1}^{N} \sigma(p_i) + \sum_{i=1}^{N-1} \sum_{j=i+1}^{N} \left[\frac{a}{2} \|p_i - p_j\|^2 + \frac{bc}{2} \exp\left(-\frac{\|p_i - p_j\|^2}{c} \right) \right] \tag{23}$$

Taking the gradient of the environment potential $\sigma(\cdot)$ in (22) at position p_i we obtain

$$\nabla_{p_i} \sigma(p_i) = -\sum_{i=1}^{N} \frac{2B_{\sigma_i}}{c_i} (p_i - x_{\sigma_i}) \exp\left(-\frac{\|p_i - x_{\sigma_i}\|^2}{c_i} \right), \tag{24}$$

which will appear in (3) together with (4) and (6). The time derivative of $\nabla_{p_i} \sigma(p_i)$, which is needed in order to calculate $\dot{\theta}_{id}$ in (21), can be obtained as

$$\frac{d}{dt}\left(\nabla_{p_i} \sigma(p_i) \right) = -\sum_{j=1}^{N} \frac{2B_{\sigma_i}}{c_i} \exp\left(-\frac{\|p_i - x_{\sigma_i}\|^2}{c_i} \right) \left[I - \frac{2}{c_i} (p_i - x_{\sigma_i})(p_i - x_{\sigma_i})^\top \right] \dot{p}_i. \tag{25}$$

Then the same procedure based on the sliding mode control technique presented in the preceding sections is applied without any modification and results similar to those in [17] are obtained for the swarm consisting of agents with non-holonomic dynamics in (1). This solves Problem 2, provided that the system parameters are chosen appropriately (as noted in [17]).

6. Formation Control

In this section we show that the procedure discussed in the previous sections can be extended to the formation control problem as well by defining pair-dependent inter-agent interactions. Formation control (i.e., achieving a predefined shape or formation and maintaining it during motion) is a relevant problem that has been considered extensively in the multi-agent coordination literature [3, 28–31, 33] and can be defined in our setting as follows.

Problem 3 (Formation Control) *Design the control inputs* $u_i = [u_{i1}, u_{i2}]^\top$ *for each agent* $A_i, i = 1, \dots N$, *such that given a predefined geometrical formation with a set of desired inter-agent distances* d_{ij}, *as* $t \to \infty$ *we have*

$$\lim_{t\to\infty} \|p_i - p_j\| = d_{ij},$$

for all pairs (i, j).

One method for achieving formations is using potential functions [16,22,30–32] and that is the approach we use. The usual approach is to define a potential function which has its global minimum at the desired formation and then design the control strategy so that the agents move along the negative gradient of the potential. However, one shortcoming of this approach is that, unless the potential function is defined such that it has a unique minimum at the desired formation, it may have several local minima and therefore it is not possible to globally guarantee acquisition of the formation and the results obtained are usually local. In this article we use the potential function (5) with pair dependent parameters a_{ij}, b_{ij}, and c_{ij} (which suffers from the above mentioned local minima problem). In other words, we have

$$J(p) = \sum_{i=1}^{N-1} \sum_{j=i+1}^{N} \left[\frac{a_{ij}}{2} \|p_i - p_j\|^2 + \frac{b_{ij} c_{ij}}{2} \exp\left(-\frac{\|p_i - p_j\|^2}{c_{ij}} \right) \right]. \tag{26}$$

Here the attraction and repulsion forces between agents A_i and A_j balance at

$$\delta_{ij} = \sqrt{c_{ij} \ln\left(\frac{b_{ij}}{a_{ij}}\right)}.$$

By choosing the parameters a_{ij}, b_{ij}, and c_{ij} such that $\delta_{ij} = d_{ij}$, where d_{ij} is the desired inter-agent distance between agents A_i and A_j at the desired formation one can guarantee that $J(p)$ has its (not necessarily unique) global minimum at the desired formation. Then, by using the procedure discussed in the preceding sections one can guarantee that the desired formation is achieved provided that at the time when sliding mode occurs on all the sliding surfaces the positions of the agents are "close enough" to the desired formation. Note, however, that the procedure is not limited to the particular potential functions considered here and can be used with other potential functions as well. In particular, by defining the potential function as in [30] such that it has a unique minimum at the desired formation and using the sliding mode control procedure discussed here one can globally guarantee achieving the desired formation.

7. Simulation Results

In this section we present simulation results to test the effectiveness of the method discussed. The potential function that we used in the simulations is the function with linear attraction and exponential repulsion given in (5).

The sliding mode control method uses the sgn function to calculate the control inputs u_{i1} and u_{i2}. Although this works very well in theory, in practice it may result in high frequency chattering (and numerical problems during simulation). There are various methods for smoothing the sliding mode control input to reduce the chattering. The analysis of such techniques is out of the scope of this article. Still however, we used the $\tanh(\gamma y)$ function instead of the the $\mathrm{sgn}(y)$ function in the simulations, where $\gamma > 0$ is a smoothness parameter.

The values of the control gains K_{i1} and K_{i2} are also very important and they need to be chosen "high enough" in order for the procedure to work properly. They also affect the reaching time to the respective sliding surfaces. The constant parameter $c > 0$ used in the definition of the sliding surface (11) which is used for orientation control determines the slope of the sliding line ($-\frac{1}{c}$ is the slope) that controls the speed of the exponential decay of $(\theta_i - \theta_{id})$ to zero after the sliding surface is reached. It provides also a smoother rotation for the agent.

We performed several simulations with different number of agents. However, since the simulations obtained for different parameters and agent numbers are in principle the same (do not differ qualitatively) here we show only the ones for $N = 10$ and potential function parameters $a = 0.01$, $b = 20$, and $c = 1$. For the aggregating swarm simulations the control input gains are chosen as $K_{i1} = K_{i2} = 10$ and the slope parameter of the orientation sliding line/surface is chosen as $c = 0.5$. The smoothness/sharpness parameter for the tanh function for both of the control inputs are chosen as $\gamma_{i1} = \gamma_{i2} = 10$. Without loss of generality the mass and the inertia of all the agents are chosen equal and in particular $m_i = 1$ and $I_i = 1$ for all $i = 1, \ldots, N$. The simulation results show that the agents aggregate as predicted by theory.

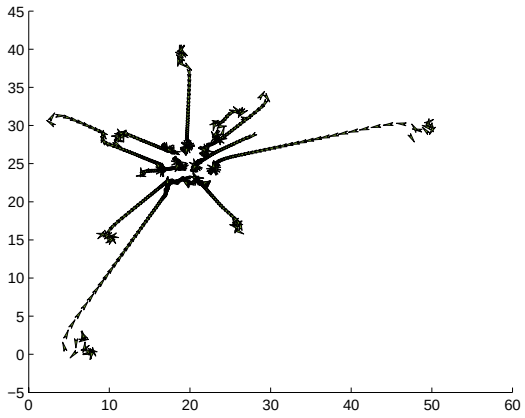

Figure 3. Trajectories of the agents of a 10-agent swarm during the aggregation process.

Figure 3 shows the motion (the trajectories) for random initial positions and orientations. The agents are plotted as polygons so that their orientations are explicitly shown. It is observed that the agents aggregate quickly and after aggregation they start to reorient themselves since there the variation of the time-varying potential function (which is due to the motion of the other agents in the group) is higher.

In Figure 4 we see the inter-member distances between robots. The curves specify the maximum, minimum and average distances between the members of the swarm. The distance decreases exponentially as expected and they converge to constant values similar to the results obtained before in [15]. For the above values of the parameters a, b and c the distance at which the attraction and repulsion between two

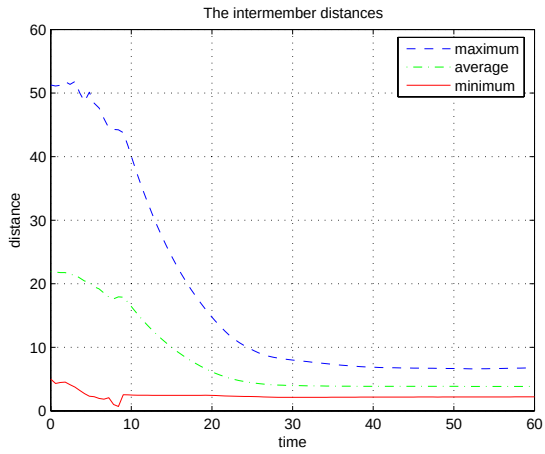

Figure 4. Inter-agent distances during the aggregation process.

individuals balance is $\delta = 2.7570$.

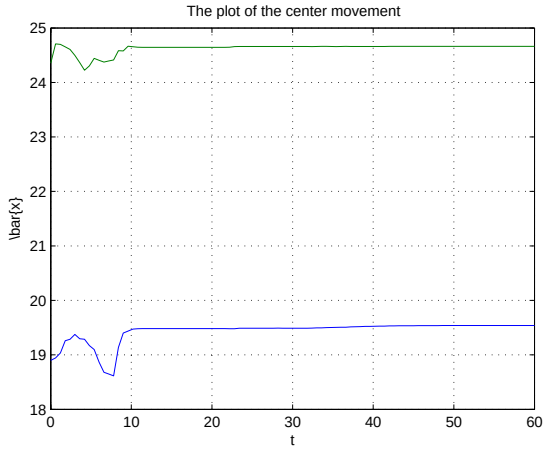

Figure 5. The x and y coordinates of the swarm center during the aggregation process.

In [15] it was shown that the centroid of the swarm will be stationary for all time. Here this is guaranteed to be the case once sliding mode occurs on all surfaces and the orientations and the speeds of all the agents converge to the desired values. Therefore, although initially the center may not be stationary, after a while it must become stationary. Figure 5 shows the plot of the center movement. Keeping in mind that we are working in 2-dimensional space, this plot shows the center movement in x-axis and y-axis. As expected after a while the location of the center converges to a constant position and stays there during the rest of the simulation.

Figure 6 is the plot of the average distance between the swarm members and the center of the swarm. The value decreases exponentially during the simulation. It is stable and smooth.

Figure 7 shows the final positions of the swarm members (shown as circles) and the center location movement (shown as stars). An interesting observation here is that at their final positions the swarm members are distributed in almost a grid-like arrangement. Also one should note that the distances between final positions of swarm members change for different values of attraction and repulsion parameters. For

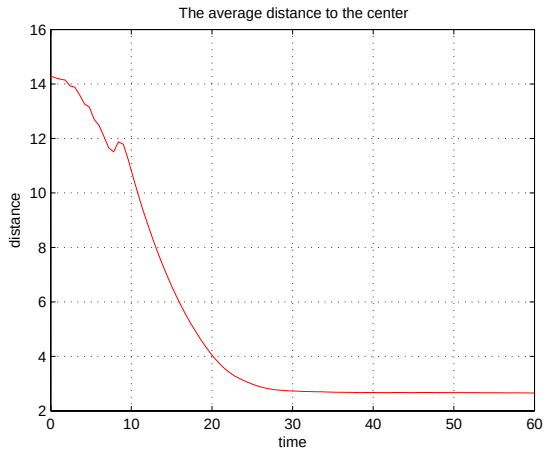

Figure 6. Average agent distance to the swarm center during the aggregation process.

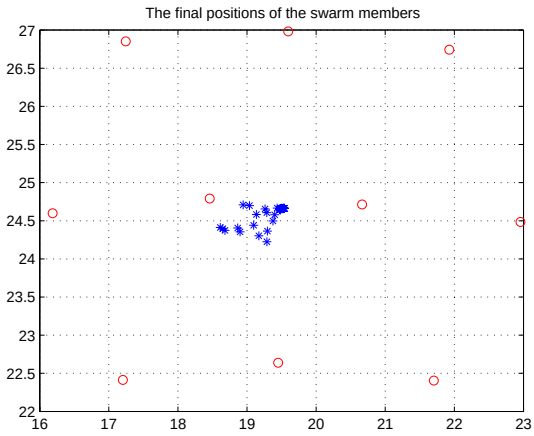

Figure 7. Final positions of the agents whose trajectories are given in Figure 3.

example, increasing the attraction parameter a or decreasing the repulsion parameter b results in decrease in the inter-agent distances at the final positions.

Figure 8 illustrates the result of the application of the method to the formation control problem. For this (formation control) simulation the control input gains are chosen as $K_{i1} = 50$ and $K_{i2} = 100$ and the slope parameter of the orientation sliding line/surface is chosen as $c = 0.05$. In this simulation a group of six agents are required to form an equilateral triangle formation. For this formation the desired inter-agent distances d_{ij} are 1, 2, or $\sqrt{3}$ depending on the relative positions of the agents in the triangle. The final positions of these agents are depicted in detail in Figure 9, where the stars show the center movement. Figure 10 shows the paths of the agents for the foraging problem. For this (foraging) simulation the control input gains are chosen as $K_{i1} = 20$ and $K_{i2} = 40$ and the slope parameter of the orientation sliding line/surface is chosen as $c = 0.05$. In this simulation we used the environmental potential (resource profile) in Figure 2. The contour curves in Figure 10 show the equipotential contours of the environmental potential. As can be seen from the figure the agents tend to move towards the minima of the profile while staying cohesive with close neighbors and avoiding maxima. Black circles indicate the initial positions of the agents

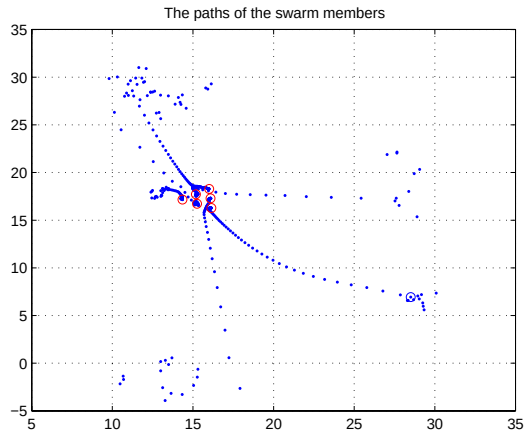

Figure 8. Paths of the agents forming a triangle formation.

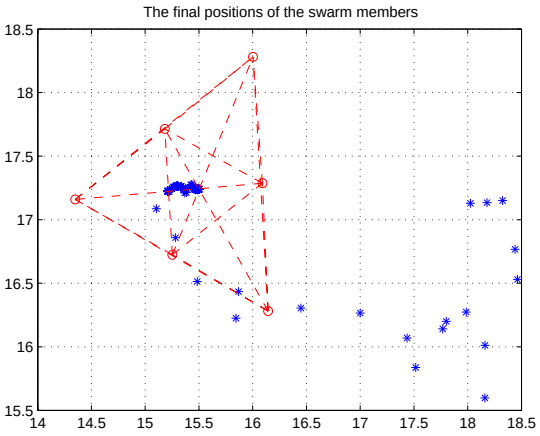

Figure 9. Final positions of the agents forming a triangle formation.

while red circles denote the final positions.

8. Concluding Remarks

In this article we have developed a strategy for aggregation of a swarm of non-holonomic agents based on artificial potential functions and the sliding mode control technique. The method is based on forcing the motion of the agents along the gradient field of the potential function generated based on the inter-individual distance requirements in the swarm aggregate. Later, using the same techniques, similar strategies have been developed for foraging and formation control of swarms in the same setting. Corresponding convergence results have been analytically established and demonstrated via simulations. The authors are currently working on application of the same approach for tracking desired trajectories or moving targets, and elaboration of the formation control results for different arbitrary desired formation geometries. A particular focus of this ongoing study is maintenance of certain geometrical formations while the centroid p_c is required to track a certain trajectory. Possible future research directions include investigation of the

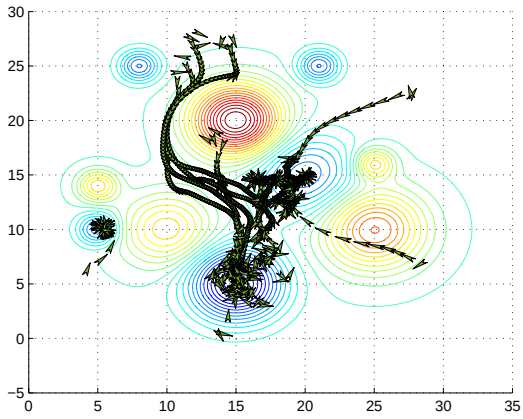

Figure 10. Path of the agents moving in the profile.

problems in this paper when the sensing radius of the agents is limited, i.e. for the case where each agent can sense the positions of the agents that are closer to it than a certain threshold. Another potential future work is experimenting the developed control schemes in real-time laboratory settings.

Appendix

Derivation of $\alpha(p)$

From (6) we have

$$\begin{aligned}
\dot{g}(p_i - p_j) &= (\dot{p}_i - \dot{p}_j)\left[a - b\exp\left(-\frac{\|p_i - p_j\|^2}{c}\right)\right] \\
&\quad +(p_i - p_j)\left[b\frac{2}{c}(p_i - p_j)^\top(\dot{p}_i - \dot{p}_j)\exp\left(-\frac{\|p_i - p_j\|^2}{c}\right)\right] \\
&= (\dot{p}_i - \dot{p}_j)\left[a - b\exp\left(-\frac{\|p_i - p_j\|^2}{c}\right)\right] \\
&\quad +b\frac{2}{c}\exp\left(-\frac{\|p_i - p_j\|^2}{c}\right)(p_i - p_j)(p_i - p_j)^\top(\dot{p}_i - \dot{p}_j) \\
&= G(p_i - p_j)(\dot{p}_i - \dot{p}_j)
\end{aligned}$$

where the 2×2 matrix $G(p_i - p_j)$ is defined as

$$G(p_i - p_j) = aI + b\exp\left(-\frac{\|p_i - p_j\|^2}{c}\right)\left(\frac{2}{c}(p_i - p_j)(p_i - p_j)^\top - I\right)$$

Then, from (4) and (6) and the expression above we have From (4),(6) and above, we have

$$\frac{d}{dt}(\nabla_{p_i} J(p)) = \begin{bmatrix} \frac{d}{dt}(J_{x_i}) \\ \frac{d}{dt}(J_{y_i}) \end{bmatrix} = \sum_{j=1, j\neq i}^{N} \dot{g}(p_i - p_j) = \sum_{j=1, j\neq i}^{N} G(p_i - p_j)(\dot{p}_i - \dot{p}_j) \tag{27}$$

for $i = 1, \ldots, N$.

Next, we derive an expression for $\alpha(p)$ for which $|\dot{v}_{id}| \leq \alpha(p)$: Using (9), assuming that the entries of $\nabla_{p_i} J(p)$ are non-zero, and implying the fact that $\|\nabla_{p_i} J(p)\| = ((\nabla_{p_i} J(p))^T \nabla_{p_i} J(p))^{1/2}$ we have

$$\begin{aligned} |\dot{v}_{id}| &= \left| \|\nabla_{p_i} J(p)\|^{-1} (\nabla_{p_i} J(p))^T \frac{d}{dt}(\nabla_{p_i} J(p)) \right| \\ &\leq \|\nabla_{p_i} J(p)\|^{-1} \|\nabla_{p_i} J(p))\| \left\| \frac{d}{dt}(\nabla_{p_i} J(p)) \right\| = \left\| \frac{d}{dt}(\nabla_{p_i} J(p)) \right\| \end{aligned}$$

Hence, using (27), we have

$$\begin{aligned} |\dot{v}_{id}| &\leq \sum_{j=1, j\neq i}^{N} \|G(p_i - p_j)\| \|\dot{p}_i - \dot{p}_j\| \leq \sum_{j=1, j\neq i}^{N} \|G(p_i - p_j)\| \left(\|\dot{p}_i\| + \|\dot{p}_j\|\right) \\ &\leq 2 \sum_{j=1, j\neq i}^{N} \|G(p_i - p_j)\| \max_{k\in\{1,\ldots,N\}} \|\dot{p}_k\| \end{aligned} \tag{28}$$

where $\|G\|$ denotes the induced 2-norm of the matrix G.

Using (1), (9), (10) we have

$$\|\dot{p}_k\| = v_k = v_{kd} + s_{v_k} = \|\nabla_{p_k} J(p)\| + s_{v_k}$$

Assuming that the control law is chosen such that (12) is satisfied, we have $s_{v_k}(t) < s_{v_k}(0)$ for any $t \geq 0$. Therefore, we have

$$\|\dot{p}_k\| \leq \|\nabla_{p_k} J(p)\| + s_{v_k}(0)$$

Substituting in (28), we obtain

$$|\dot{v}_{id}| \leq \alpha(p)$$

where

$$\begin{aligned} \alpha(p) &= 2\bar{\alpha}(p) \max_{i\in\{1,\ldots,N\}} \left(\sum_{j=1, j\neq i}^{N} \|G(p_i - p_j)\| \right), \\ \bar{\alpha}(p) &= \max_{k\in\{1,\ldots,N\}} \left(\|\nabla_{p_k} J(p)\| + s_{v_k}(0)\right) \end{aligned}$$

References

[1] C. W. Reynolds, "Flocks, herds, and schools: A distributed behavioral model," *Comp. Graph.*, vol. 21, no. 4, pp. 25–34, 1987.

[2] H. Yamaguchi, "A cooperative hunting behavior by mobile-robot troops," *The International Journal of Robotics Research*, vol. 18, no. 8, pp. 931–940, September 1999.

[3] J. P. Desai, J. Ostrowski, V. Kumar, "Modeling and control of formations of nonholonomic mobile robots," *IEEE Trans. on Robotics and Automation*, vol. 17, no. 6, pp. 905–908, December 2001.

[4] J.M. Fowler, R. D'Andrea, "A formation flight experiment," *IEEE Control Systems Magazine*, vol. 23, no. 5, pp. 35–43, 2003.

[5] W. Ren, R.W. Beard, "A decentralized scheme for spacecraft formation flying via the virtual structure approach," *AIAA Journal of Gudiance, Control and Dyanmics*, vol. 27, no. 1, pp. 73–82, 2004.

[6] D.J. Stilwell, B.E. Bishop, C.A. Sylvester, "Redundant manipulator techniques for partially decentralized path planning and control of a platoon of autonomous vehicles," *IEEE Transactions on Systems Man and Cybernetics Part B-Cybernetics*, vol. 35, no. 4, pp. 842–848, 2005.

[7] J. Cortes, S. Martinez, T. Karatas, F. Bullo, "Coverage control for mobile sensing networks," *IEEE Trans. on Robotics and Automation*, vol. 20, no. 2, pp. 243–255, 2004.

[8] I. F. Akyıldız, W. Su, Y. Sankarasubramniam, E. Çayırcı, "A survey on sensor networks," *IEEE Commununi-cations Magazine*, vol. 40, no. 8, pp. 102–114, August 2002.

[9] V. Gazi, B. Fidan, "Coordination and control of multi-agent dynamic systems: Models and approaches," in *Proceedings of the SAB06 Workshop on Swarm Robotics Swarm Robotics*, E. Sahin, W. M. Spears, A. F. T. Winfield, Eds., Lecture Notes in Computer Science (LNCS) 4433, pp. 71–102. Springer-Verlag, Berlin Heidelberg, 2007.

[10] J. K. Parrish, W. M. Hamner, Eds., *Animal Groups in Three Dimensions*, Cambridge University Press, 1997.

[11] C. M. Breder, "Equations descriptive of fish schools and other animal aggregations," *Ecology*, vol. 35, no. 3, pp. 361–370, 1954.

[12] A. Okubo, "Dynamical aspects of animal grouping: swarms, schools, flocks, and herds," *Advances in Biophysics*, vol. 22, pp. 1–94, 1986.

[13] K. Warburton, J. Lazarus, "Tendency-distance models of social cohesion in animal groups," *Journal of Theoretical Biology*, vol. 150, pp. 473–488, 1991.

[14] D. Grünbaum, A. Okubo, "Modeling social animal aggregations," in *Frontiers in Theoretical Biology*, vol. 100 of *Lecture Notes in Biomathematics*, pp. 296–325. Springer-Verlag, New York, 1994.

[15] V. Gazi, K. M. Passino, "Stability analysis of swarms," *IEEE Trans. on Automatic Control*, vol. 48, no. 4, pp. 692–697, April 2003.

[16] V. Gazi, K. M. Passino, "A class of attraction/repulsion functions for stable swarm aggregations," *Int. J. Control*, vol. 77, no. 18, pp. 1567–1579, December 2004.

[17] V. Gazi, K. M. Passino, "Stability analysis of social foraging swarms," *IEEE Trans. on Systems, Man, and Cybernetics: Part B*, vol. 34, no. 1, pp. 539–557, February 2004.

[18] Y. Liu, K. M. Passino, "Stable social foraging swarms in a noisy environment," *IEEE Transactions on Automatic Control*, vol. 49, no. 1, pp. 30–44, 2004.

[19] Y. Liu, K. M. Passino, M. M. Polycarpou, "Stability analysis of one-dimensional asynchronous swarms," *IEEE Trans. on Automatic Control*, vol. 48, no. 10, pp. 1848–1854, October 2003.

[20] Y. Liu, K. M. Passino, M. M. Polycarpou, "Stability analysis of m-dimensional asynchronous swarms with a fixed communication topology," *IEEE Trans. on Automatic Control*, vol. 48, no. 1, pp. 76–95, January 2003.

[21] V. Gazi, K. M. Passino, "Stability of a one-dimensional discrete-time asynchronous swarm," *IEEE Trans. on Systems, Man, and Cybernetics: Part B*, vol. 35, no. 4, pp. 834–841, August 2005.

[22] V. Gazi, "Swarm aggregations using artificial potentials and sliding mode control," *IEEE Trans. on Robotics*, vol. 21, no. 6, pp. 1208–1214, December 2005.

[23] N. E. Leonard, E. Fiorelli, "Virtual leaders, artificial potentials and coordinated control of groups," in *Proc. Conf. Decision Contr.*, Orlando, FL, December 2001, pp. 2968–2973.

[24] R. Bachmayer, N. E. Leonard, "Vehicle networks for gradient descent in a sampled environment," in *Proc. Conf. Decision Contr.*, Las Vegas, Nevada, December 2002, pp. 112–117.

[25] O. Khatib, "Real-time obstacle avoidance for manipulators and mobile robots," *The International Journal of Robotics Research*, vol. 5, no. 1, pp. 90–98, 1986.

[26] E. Rimon, D. E. Koditschek, "Exact robot navigation using artificial potential functions," *IEEE Trans. on Robotics and Automation*, vol. 8, no. 5, pp. 501–518, October 1992.

[27] J. H. Reif, H. Wang, "Social potential fields: A distributed behavioral control for autonomous robots," *Robotics and Autonomous Systems*, vol. 27, pp. 171–194, 1999.

[28] J. P. Desai, J. Ostrowski, V. Kumar, "Controlling formations of multiple mobile robots," in *Proc. of IEEE International Conference on Robotics and Automation*, Leuven, Belgium, May 1998, pp. 2864–2869.

[29] P. Ögren, M. Egerstedt, X. Hu, "A control Lyapunov function approach to multi-agent coordination," in *Proc. Conf. Decision Contr.*, Orlando, FL, December 2001, pp. 1150–1155.

[30] M. Egerstedt, X. Hu, "Formation constrained multi-agent control," *IEEE Trans. on Robotics and Automation*, vol. 17, no. 6, pp. 947–951, December 2001.

[31] R. Olfati-Saber, R. M. Murray, "Distributed cooperative control of multiple vehicle formations using structural potential functions," in *Proc. IFAC World Congress*, Barcelona, Spain, June 2002.

[32] P. Ögren, E. Fiorelli, N. E. Leonard, "Formations with a mission: Stable coordination of vehicle group maneuvers," in *Symposium on Mathematical Theory of Networks and Systems*, August 2002.

[33] J. R. T. Lawton, R. W. Beard, B. J. Young, "A decentralized approach to formation maneuvers," *IEEE Trans. on Robotics and Automation*, vol. 19, no. 6, pp. 933–941, December 2003.

[34] R. Olfati-Saber, "Flocking for multi-agent dynamic systems: Algorithms and theory," *IEEE Trans. on Automatic Control*, vol. 51, no. 3, pp. 401–420, March 2006.

[35] H. G. Tanner, A. Jadbabaie, G. J. Pappas, "Stable flocking of mobile agents, part i: Fixed topology," in *Proc. Conf. Decision Contr.*, Maui, Hawaii, December 2003, pp. 2010–2015.

[36] H. G. Tanner, A. Jadbabaie, G. J. Pappas, "Stable flocking of mobile agents, part ii: Dynamic topology," in *Proc. Conf. Decision Contr.*, Maui, Hawaii, December 2003, pp. 2016–2021.

[37] H. G. Tanner, A. Jadbabaie, G. J. Pappas, "Flocking in teams of nonholonomic agents," in *Cooperative Control*, N.E. Leonard V.J. Kumar and A.S. Morse, Eds. 2005, vol. 309 of *Lecture Notes in Control and Information Sciences*, pp. 229–239, Springer-Verlag.

[38] V. I. Utkin, *Sliding Modes in Control and Optimization*, Springer Verlag, Berlin, Heidelberg, 1992.

[39] V. I. Utkin, S. V. Drakunov, H. Hashimoto, F. Harashima, "Robot path obstacle avoidance control via sliding mode approach," in *IEEE/RSJ International Workshop on Intelligent Robots and Systems*, Osaka, Japan, November 1991, pp. 1287–1290.

[40] J. Guldner, V. I. Utkin, "Sliding mode control for an obstacle avoidance strategy based on an harmonic potential field," in *Proc. Conf. Decision Contr.*, San Antonio, Texas, December 1993, pp. 424–429.

[41] J. Guldner, V. I. Utkin, "Sliding mode control for gradient tracking and robot navigation using artificial potential fields," *IEEE Trans. on Robotics and Automation*, vol. 11, no. 2, pp. 247–254, April 1995.

[42] J. Guldner, V. I. Utkin, "Stabilization on non-holonimic mobile robots using lyapunov functions for navigation and sliding mode control," in *Proc. Conf. Decision Contr.*, Lake Buena Vista, Florida, December 1994, pp. 2967–2972.

[43] J. Guldner, V. I. Utkin, H. Hashimoto, F. Harashima, "Tracking gradients of artificial potential fields with non-holonomic mobile robots," in *Proc. American Control Conf.*, Seattle, Washington, June 1995, pp. 2803–2804.

[44] J. Guldner, V. I. Utkin, "Tracking the gradient of artificial potential fields: Sliding mode control for mobile robots," *Int. J. Control*, vol. 63, no. 3, pp. 417–432, 1996.

[45] D. Grünbaum, "Schooling as a strategy for taxis in a noisy environment," *Evolutionary Ecology*, vol. 12, pp. 503–522, 1998.